DESIGN OF A 60 GHz BEAM WAVEGUIDE ANTENNA POSITIONER

Kenneth S. Emerick*

ABSTRACT

This paper presents a development model antenna positioner mechanism with an integral 60 GHz radio frequency (RF) beam waveguide. The system features a 2-ft diameter carbon-fiber reinforced epoxy antenna reflector and support structure, and a 2-degree-of-freedom (DOF) elevation over azimuth mechanism providing hemispherical field of view. The paper focuses on the constraints imposed on the mechanism by the RF subsystem and how they impacted the mechanical configuration. A description of the system hardware and performance characteristics will be presented. A discussion and comparison of alternative antenna mechanism configurations will also be given. The paper concludes with the presentation of experimental results, a summary, and conclusions.

BACKGROUND

The desire to have satellite communication links at frequencies of 60 GHz is driven by a number of factors. The high frequency reduces beamwidth, making the system more jam resistant. The system is less likely to cause interference with other systems operating in the vicinity. Finally, for a given antenna size, higher data rates can be supported, leading to a lighter, more compact design.

In a conventional RF system, an arrangement of waveguide tubing and rotary joints takes the RF energy from the feed to the transponder electronics, which are mounted on or near the spacecraft to provide them with a hospitable environment. However, using waveguide tubing at 60 GHz results in a loss of approximately 1 dB/ft. Each rotary joint adds an additional loss of approximately 1 dB. A 2-DOF elevation over azimuth antenna positioner with two rotary joints and one foot of waveguide would lose 50 percent of its RF signal strength in the waveguide system.

The system shown in Figure 1 is a method of transferring the RF energy to the transponder electronics in a more efficient manner. The RF energy transmitted by the feed is directed to the reflector by means of the beam waveguide assembly. The beam waveguide is a series of steerable RF mirrors which reflect and focus the beam as it crosses the axes of rotation. This allows the antenna feed and associated electronics to remain stationary while the reflector is tracking or acquiring a target. One of the mirrors (M1) is a planer, while the other three are elliptically contoured in order to focus the

*Ford Aerospace Corporation, Palo Alto, California.

beam. The angle of incidence between the mirror and beam center is 45 deg, making the total angle through which the beam is reflected at each mirror equal to 90 deg. The beam waveguide has a projected loss of less than 0.5 dB. Our system has four mirrors arranged as shown in Figure 1. However, other configurations having different numbers of mirrors are possible.

SYSTEM REQUIREMENTS

The pointing error requirements are defined by the signal beamwidth, and assembly tolerances are defined by both the beamwidth and frequency. Ten percent of the beamwidth is allotted for the total antenna pointing error. This system, with a 0.2 deg beamwidth, has a total pointing error budget of 0.02 deg.

The acceptable assembly and alignment tolerances are related to the wavelength, similar to optical systems, and a total positional tolerance of lambda/20 will ensure minimal losses. A 60 GHz signal has a wavelength of approximately 0.2 in., giving the system a positional tolerance of 0.010 in. This number represents the maximum true-position error that the RF centerline can deviate with respect to the focussing element optical centers, and is comprised of element manufacturing tolerances, element translational and rotational mounting errors, and system structural and thermal deflections. The location of the element in a plane perpendicular to the direction of wave propagation is crucial, as most elements are both non-planer and aspherical. As testing of the system occurred in a 1-g environment, with no offloading mechanism, structural deflections for all mechanism positions must also be within the pointing error and alignment tolerances.

The development model positioner mechanism provides hemispherical coverage with an elevation over azimuth configuration (see Fig. 2a). This configuration has a "gimbal lock," or mechanism singularity, located at the center of the mechanism pointing range, at the zenith location. The theoretical antenna tracking rates approach infinity as a target passes through this location. In practice, a circular "keyhole" region is defined by the target angular velocity, and maximum positioner angular velocity and acceleration. If the keyhole region is much smaller than the antenna beamwidth, very little signal degradation will occur. A computer program was written to analyze keyhole size as a function of the beamwidth, maximum gimbal velocities, and accelerations. The keyhole size for this system is 0.02 deg for a target moving at 1 deg/sec, and is much smaller than the beamwidth of 0.2 deg. An alternative antenna mechanism, with an X-Y configuration, would have two keyhole locations on the hemispherical field of view horizon (see Fig. 2b). This configuration may be preferable if very high tracking rates near the gimbal lock location are anticipated. The current configuration is applicable for most low-earth orbit and geostationary aircraft.

Stray RF reflections within the beam waveguide structure can also cause signal degradation. Any apertures or surfaces that may potentially reflect stray RF energy must be at a location where the RF intensity is at least 60 dB below the reference level. Unlike a typical optical system, the shape of the

beam edges cannot be accurately modelled using linear ray tracing techniques (see Fig. 3). When the beam diameter of a system approaches the wavelength, both the signal intensity across the wavefront and the diameter of the beamwaist as a function of propagation distance from a focussing element, can be represented by a gaussian function.

The beam intensity at an aperture or potentially reflective surface may be found and compared to the specification. Table 1 summarizes the system performance goals.

HARDWARE DESCRIPTION

Figure 4 shows the configuration selected for the beam waveguide mechanism. The main structure of the assembly is constructed using carbon-fiber reinforced graphite sandwich panels with an aluminum honeycomb core. Precision inserts are used to locate and align the critical RF components and the axes of rotation. The box shape of the structure makes it extremely rigid, while providing an unobstructed path for the RF energy. Note that there are no loss-producing apertures within the main structure, and only one aperture on the reflector which, as will be shown later, has an insignificant effect on system performance.

Figure 5 illustrates the layout of the positioner mechanism and the axes of rotation. Note that the elevation and azimuth axes have $\pm$90 deg and $\pm$180 deg, respectively, achieving a hemispherical field of view. Each axis is rotated by an assembly consisting of a drive actuator and position encoder. The signal path through the beam waveguide is illustrated, as is the location of the major waveguide components. Figure 6 is a photograph of the completed assembly with a reflector and sub-reflector mounted.

Alignment of the critical RF components was accomplished with precision tooling and careful measurement of the components themselves (see Fig. 7). Each component has a series of tooling balls with known locations with respect to the RF aspherical surface. No adjustments of the components were performed beyond the initial assembly.

The drive actuator selected for use in the development model is a Schaeffer Magnetics Type 5 rotary actuator. Flight models with small antennas will also use the Type 5. With larger antennas (such as a 4-m reflector), a Type 6 unit from the same manufacturer may be required. These actuators feature a permanent magnet stepper motor with a harmonic drive gear (cup type), resulting in a gearing system combining very small output step sizes with zero backlash (a characteristic of the cup-type harmonic drive). The actuator output shaft is supported by large-diameter angular contact duplex bearings, providing high load capacity and stiffness for the output shaft in radial, axial, and moment loading.

The Type 5 actuator consists of a 1.5-deg stepper motor with a 200:1 harmonic drive reduction. This production unit is modified to provide mounting locations for a Farrand Inductosyn rotary encoder. A shaft and

bearing set has also been provided to couple the encoder rotor to the output flange. Table 2 summarizes the actuator's operational characteristics. Figure 8 shows the actuator assembly.

Position encoding is provided by a Farrand Inductosyn, an inductively-coupled rotary-absolute position transducer. The device consists of a rotor and stator, with the relative position between the two providing a variation in inductance which is detected by the position readout electronics. The inductance variation is converted to a digital signal which can provide resolution up to 2^{19} bits per revolution. However, 2^{16} bits of resolution is adequate for this mechanism. The accuracy requirement is of a similar order. For the development model tests the electronics modules are non-redundant commercial quality units, as is the rotor and stator. However, upgrading the mechanical components to a flight status will require few if any design changes.

The stator is attached to the outside of the rear actuator housing. An angular contact bearing mounted in the back of the actuator provides support for the shaft that couples the Inductosyn rotor to the actuator output face. In this configuration, a gap of approximately 0.005 in. exists between the rotor and stator. An acceptable gap is maintained for all system conditions including vibration testing. The unit's diameter is slightly smaller than that of the actuator, with a total thickness of less than 0.5 in., allowing a very compact overall configuration. Note that the rotor has two pairs of cables protruding from its top surface, necessitating a rotary signal transfer assembly.

MATERIAL SELECTION AND ANALYSIS

Testing of the development model will occur in a 1-g environment, making analysis of the structural rigidity of the mechanism and comparison of the results with system alignment tolerances necessary. External loads to the mechanism will depend on the orientation of the 2-DOF mechanism. The deflection tolerances for the structure are driven by the requirement that the beam deflect less than 0.01 in. and 0.1 deg as it travels through the waveguide.

The finite element method was used to analyze the structure. the structural members of the positioner have been modeled with a combination of plate and brick elements to represent the composite sandwich. Brick elements represent the shear properties and compressive stiffness of the core, while remaining flexible in bending. Plate elements on either side of the core represent the composite faceskins. The actuators were modeled using stiffness matrix elements. The entire model contains 731 nodes and 956 elements.

The mechanism was analyzed for deflection under 1-g loading in three orthogonal directions to determine orientations of the mechanism which result in deflection maxima. After processing, a complete listing of nodal deflections is produced, which may be edited to show specific areas of interest. A sample deflection output for the reflector is shown in Table 3.

Stresses in the structure are typically under 10 psi, and the maximum deflections are well below system alignment tolerances.

Analyses of the gimbal structure were performed using a variety of materials. A composite sandwich structure with carbon-fiber reinforced graphite epoxy faceskins and an aluminum honeycomb core was selected on the basis of its high stiffness, low weight, and low thermal distortion. While not all of these properties are specifically required for testing the development model, the use of these materials will best simulate the flight hardware.

The faceskin material selected, Pitch 75, is an acceptable compromise of the above parameters, has adequate strength, and is a material with which Ford Aerospace Corporation has experience. A six-ply balanced weave was chosen for the faceskins of the structural members. This resulted in relatively isotropic material properties for the skin, which is required because the load orientation varies as the mechanism is moved. Aluminum honeycomb material with a cell size of 0.125 in. and a weight density of 2 lb/ft^3 was chosen for the core. A summary of the properties of the faceskin material is shown in Table 4.

To reduce RF reflections from the gimbal structural components, a minimum clearance of 1 in. is maintained between the 4.75-in. diameter RF path and the mechanism. A computer program was written in 1987 to analyze the signal intensity of the beam at all locations along the signal path. Our analysis of the mechanism shows signal levels of less than -80 dB at surfaces which could potentially reflect RF energy, below the level needed to introduce significant losses into the system. In addition, efforts have been made to minimize the number of possible reflecting surfaces at locations along the waveguide. As a result, the signal path is completely enclosed at only one location for approximately 0.5 in. of travel. The RF energy at this point is -120 dB. No other apertures exist in the waveguide.

PERFORMANCE RESULTS

System testing consisted of measuring sum and difference patterns at several mechanism positions. Figure 9 summarizes the test results.

Theoretical performance is almost identical to the measured performance for the beam waveguide system. At the sum signal peak, only 0.2 dB difference between theoretical and measured signal amplitude was observed. The difference signal is also very sharply defined. The total system loss is less than 0.2 dB for the sum pattern, and 0.3 dB for the difference pattern.

SUMMARY/CONCLUSIONS

Design, analysis, fabrication, and testing of a two-axis positioner mechanism with an integral beam waveguide has been successfully completed.

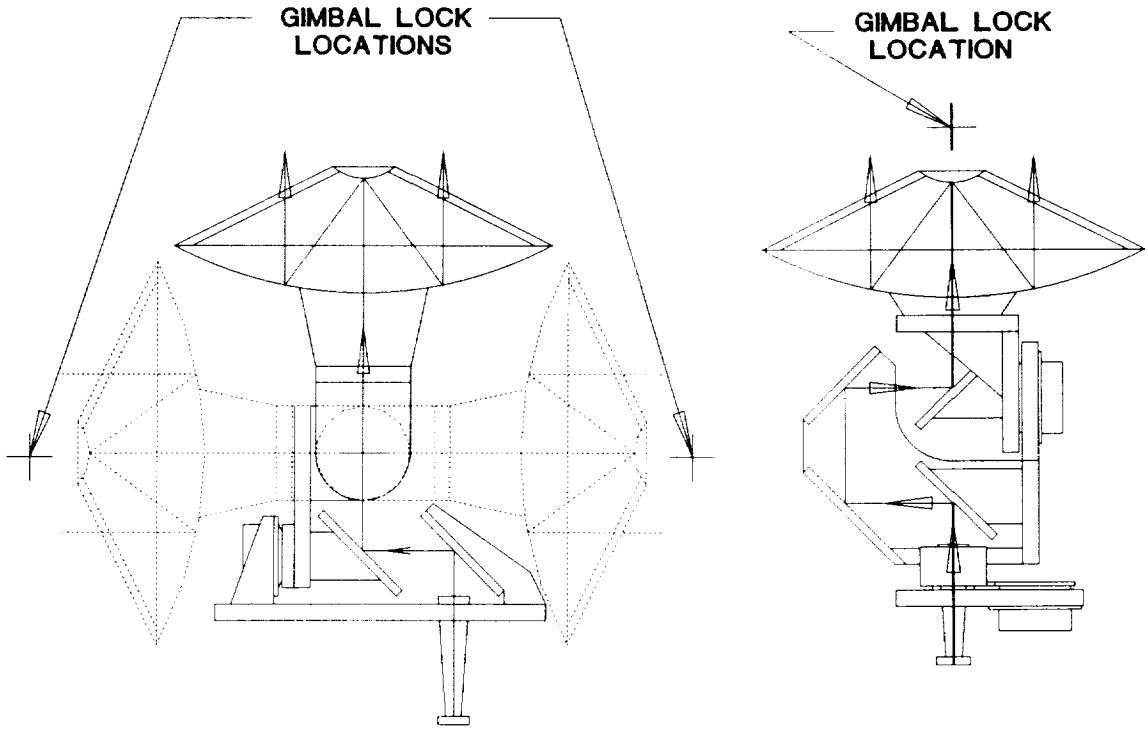

a) Az-El system b) X-Y system

Figure 2. Gimbal lock locations depend on mechanism configuration.

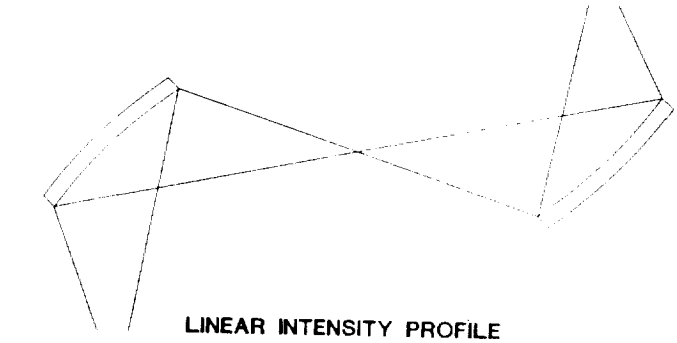

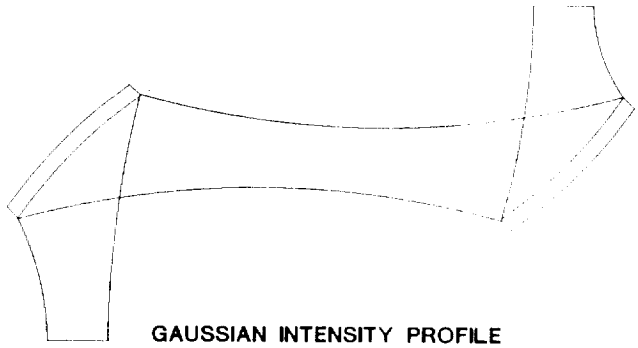

Figure 3. RF systems are best modelled assuming a gaussian intensity profile.

Stresses in the structure are typically under 10 psi, and the maximum deflections are well below system alignment tolerances.

Analyses of the gimbal structure were performed using a variety of materials. A composite sandwich structure with carbon-fiber reinforced graphite epoxy faceskins and an aluminum honeycomb core was selected on the basis of its high stiffness, low weight, and low thermal distortion. While not all of these properties are specifically required for testing the development model, the use of these materials will best simulate the flight hardware.

The faceskin material selected, Pitch 75, is an acceptable compromise of the above parameters, has adequate strength, and is a material with which Ford Aerospace Corporation has experience. A six-ply balanced weave was chosen for the faceskins of the structural members. This resulted in relatively isotropic material properties for the skin, which is required because the load orientation varies as the mechanism is moved. Aluminum honeycomb material with a cell size of 0.125 in. and a weight density of 2 lb/ft^3 was chosen for the core. A summary of the properties of the faceskin material is shown in Table 4.

To reduce RF reflections from the gimbal structural components, a minimum clearance of 1 in. is maintained between the 4.75-in. diameter RF path and the mechanism. A computer program was written in 1987 to analyze the signal intensity of the beam at all locations along the signal path. Our analysis of the mechanism shows signal levels of less than -80 dB at surfaces which could potentially reflect RF energy, below the level needed to introduce significant losses into the system. In addition, efforts have been made to minimize the number of possible reflecting surfaces at locations along the waveguide. As a result, the signal path is completely enclosed at only one location for approximately 0.5 in. of travel. The RF energy at this point is -120 dB. No other apertures exist in the waveguide.

PERFORMANCE RESULTS

System testing consisted of measuring sum and difference patterns at several mechanism positions. Figure 9 summarizes the test results.

Theoretical performance is almost identical to the measured performance for the beam waveguide system. At the sum signal peak, only 0.2 dB difference between theoretical and measured signal amplitude was observed. The difference signal is also very sharply defined. The total system loss is less than 0.2 dB for the sum pattern, and 0.3 dB for the difference pattern.

SUMMARY/CONCLUSIONS

Design, analysis, fabrication, and testing of a two-axis positioner mechanism with an integral beam waveguide has been successfully completed.

Performance of the system successfully addresses the issue of low-loss high-frequency RF transmission systems in a compact, 2-DOF mechanism with a hemispherical field of view.

The mechanism is a development model, and while further work will be needed to space-qualify the system, all major components and materials are well suited for that environment. Additional work will be required to ascertain that the system will survive launch loads, and that thermal deformations do not significantly degrade RF performance.

The elevation-azimuth mechanism configuration is acceptable for most applications. However, keyholes or mechanism singularities may restrict performance when high tracking rates with a narrow beamwidth that pass near the zenith location are required. For these applications, a third DOF or an X-Y mechanism may be needed.

The stepper motors caused excitation of system resonances. Further investigation of this effect on signal integrity should be investigated. This undesirable excitation can be reduced by replacement of the stepper units with brushless dc motors. However, this will result in more complex servo electronics.

TABLE 1. SYSTEM PERFORMANCE GOALS

Mechanism configuration	Elevation/Azimuth
Field of view	Hemispherical
Frequency	60 GHz
RF transmission method	Beam Waveguide
Beamwidth	0.2 deg
Pointing accuracy	0.02 deg
Resolution	0.01 deg
"Waveguide" insertion loss	<0.5 dB
1-g deflection	<0.01 deg
	<0.005 in.

TABLE 2. TYPE 5 ACTUATOR PERFORMANCE SUMMARY

Step size	0.0075 deg
Torsional stiffness	15000 in.-lb/rad
Axial stiffness	415000 lb/in.
Moment stiffness	325000 in.-lb/rad
Nominal output torque	600 in.-lb
Power consumption	<15 W
Weight	4.7 lb maximum
Step rate	300 Hz maximum
Bearing lubrication	Brayco 601 grease

TABLE 3. ANALYSIS RESULTS SUMMARY

	Translations			Rotations		
Load	X (in.)	Y (in.)	Z (in.)	X (deg)	Y (deg)	Z (deg)
X	1.55E-03	-2.34E-09	1.36E-09	-4.90E-10	3.14E-05	2.43E-03
Y	-4.15E-09	6.04E-04	-1.54E-04	-1.89E-05	2.47E-10	-9.90E-09
Z	2.46E-09	-3.33E-05	1.83E-04	-9.51E-06	1.38E-10	7.80E-10

TABLE 4. MATERIAL MECHANICAL PROPERTIES

Material	Tensile Modulus (MSI)	Tensile Strength (MSI)	Flex Modulus (MSI)	Flex Strength (MSI)	Density lb./in.^{3}	CTE 10^{-6} in./in.*F
Pitch 75	16.0	34.8	14.5	42.0	0.06	-0.2

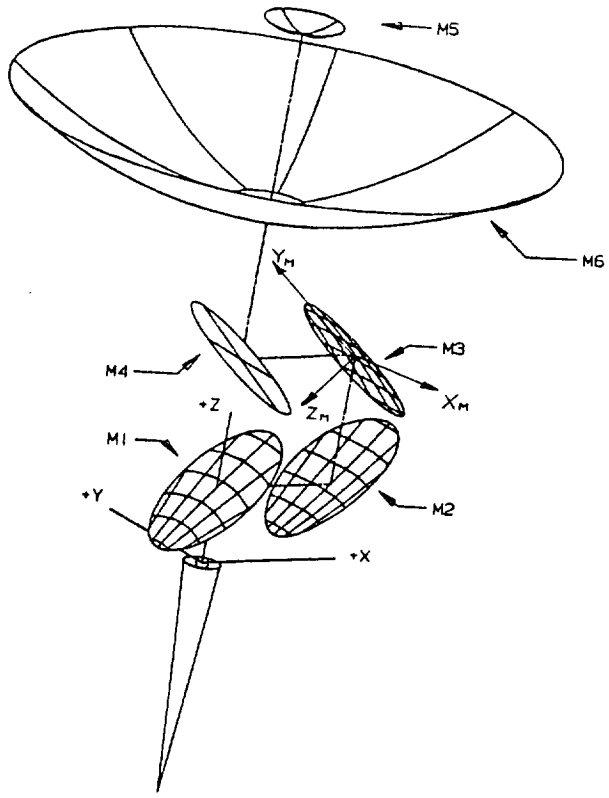

Figure 1. Beam waveguides provide a means of low-loss RF signal transfer.

C-3

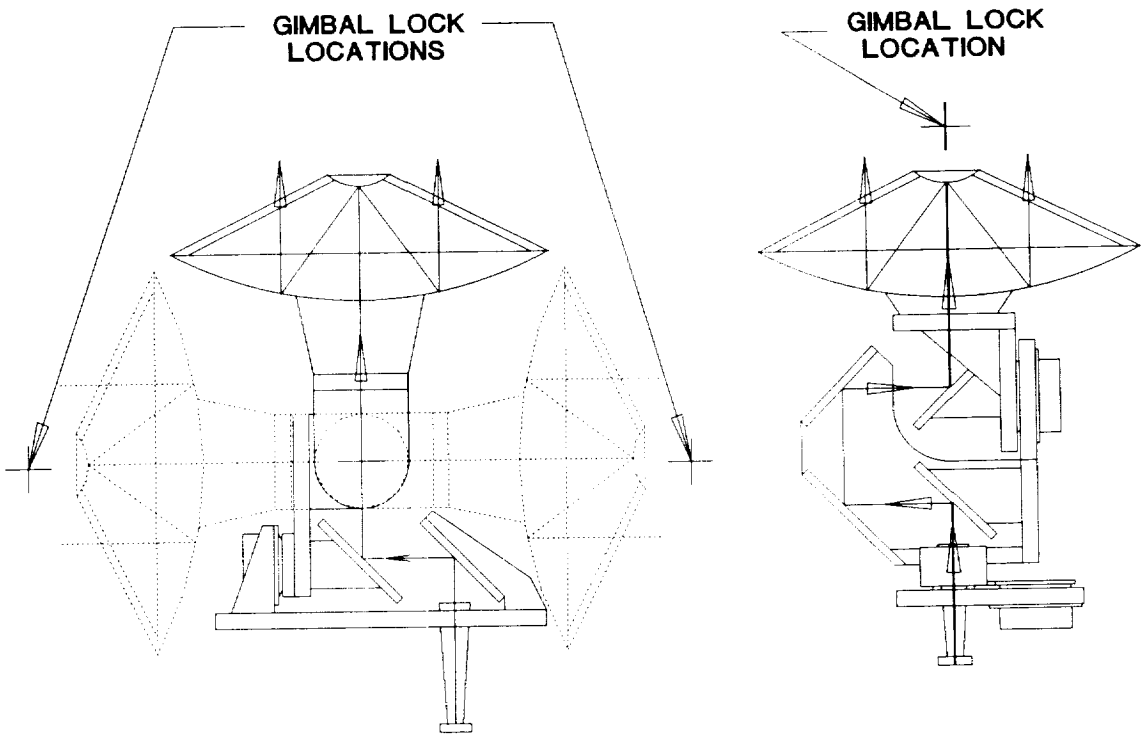

a) Az-El system

b) X-Y system

Figure 2. Gimbal lock locations depend on mechanism configuration.

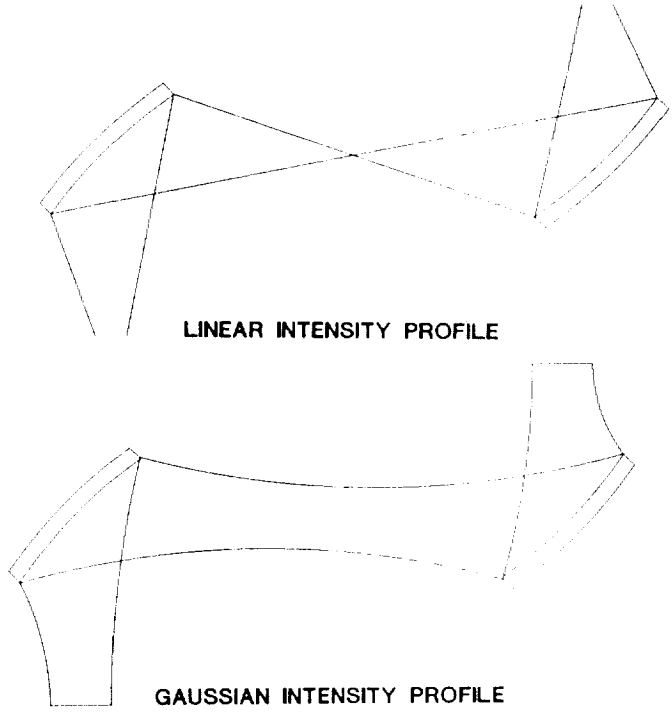

Figure 3. RF systems are best modelled assuming a gaussian intensity profile.

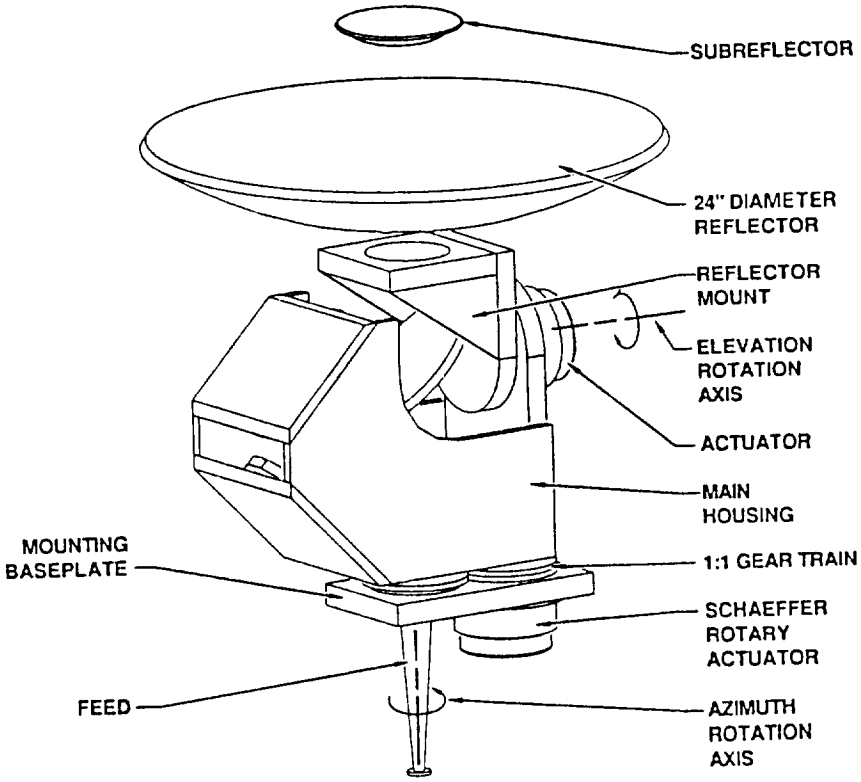

Figure 4. Beam waveguide housing, reflector, and subreflector.

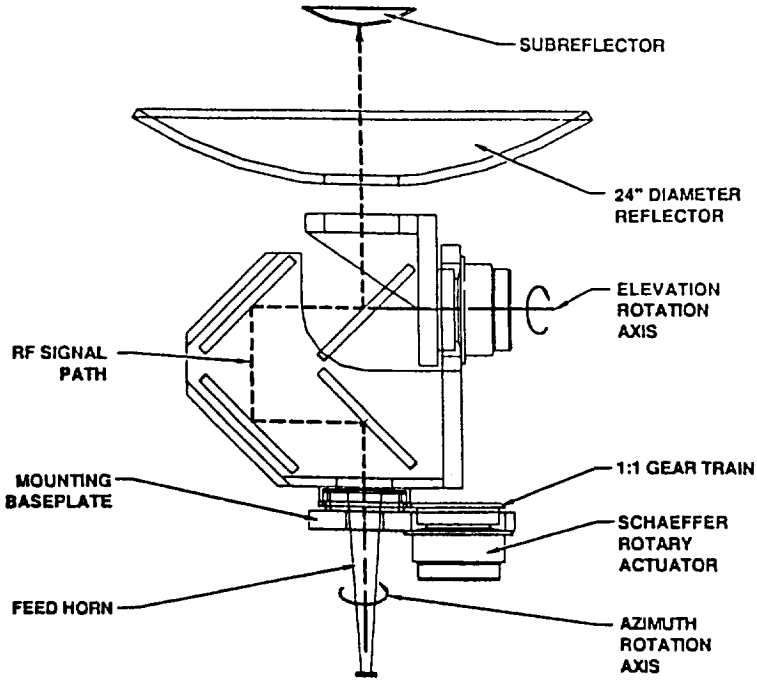

Figure 5. Mechanism cross section.

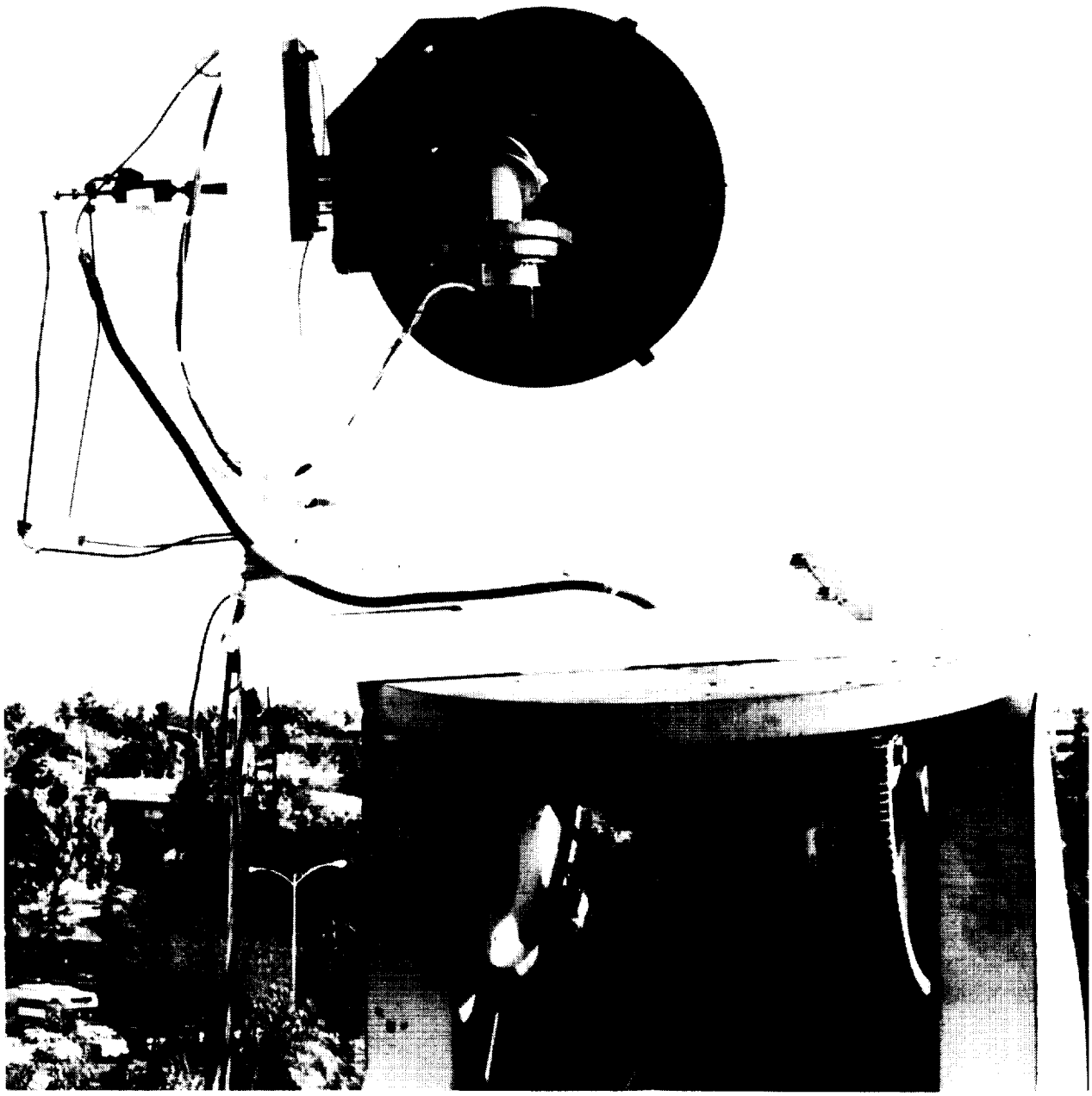

Figure 6. The beam waveguide is mounted to a range fixture for system tests.

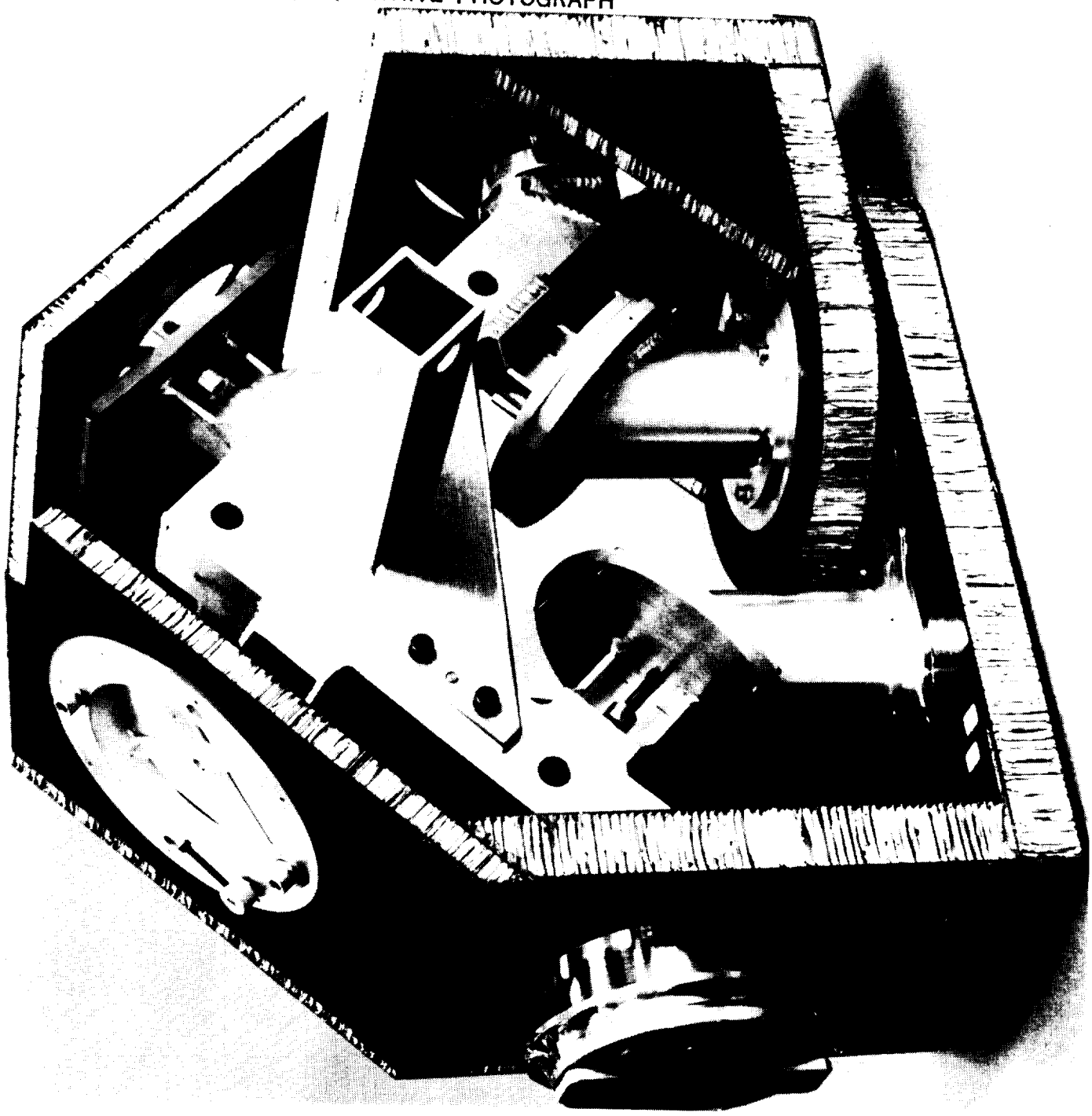

Figure 7. Precision tooling maintains system alignment during the assembly process.

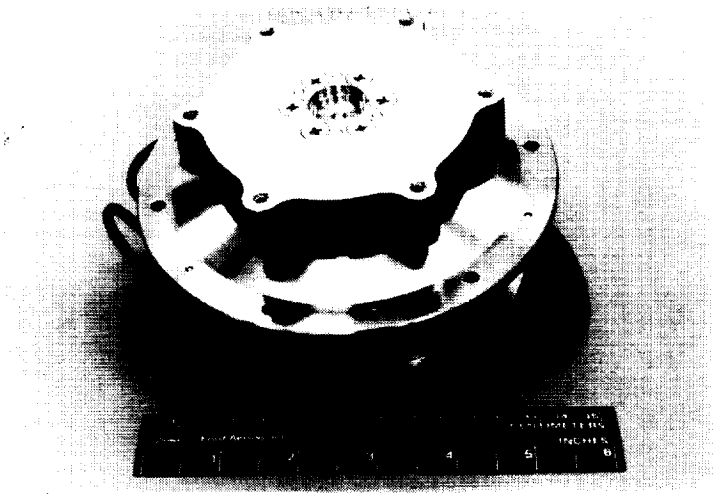

Figure 8. The Schaeffer actuators are space-proven designs.

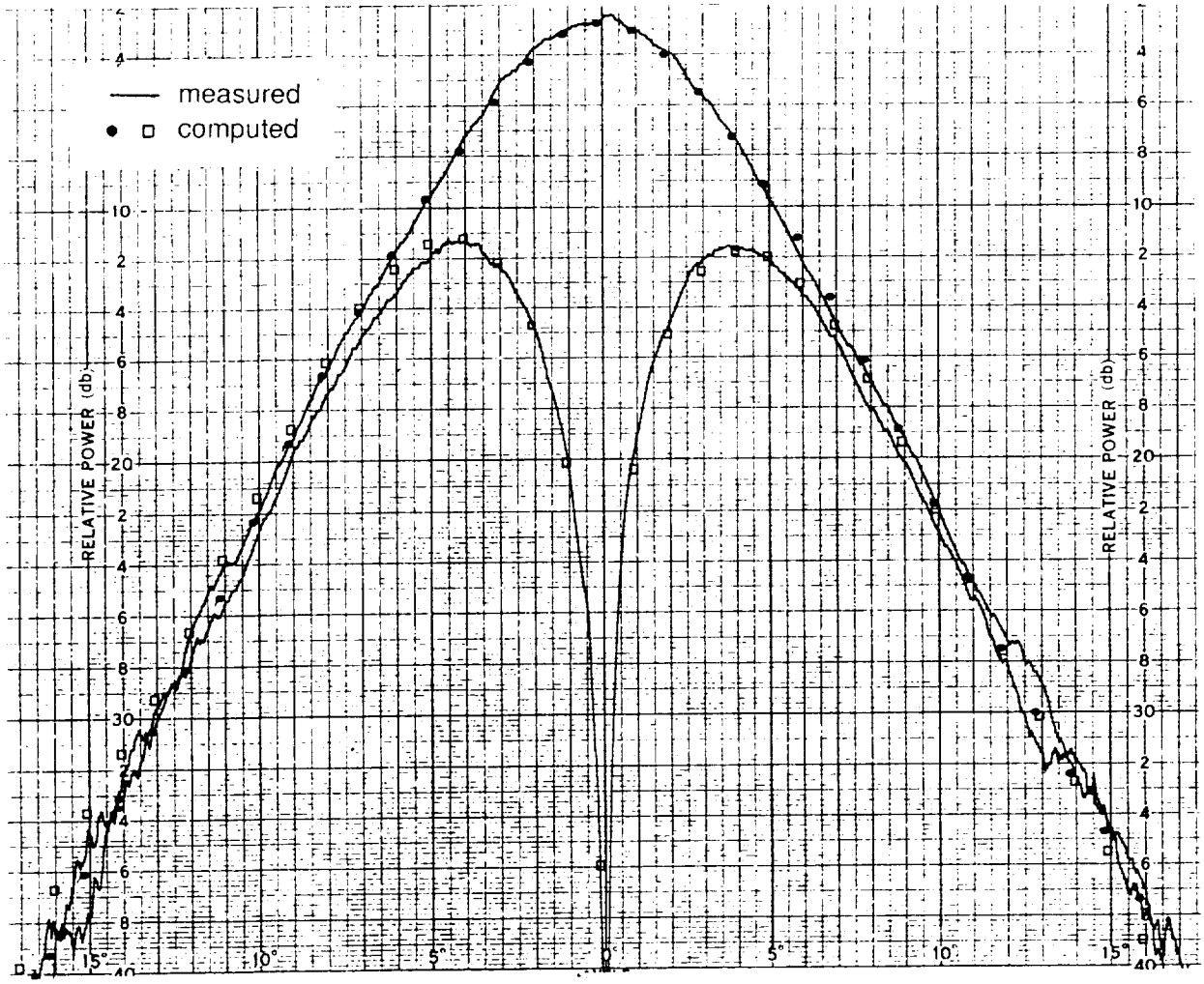

Figure 9. Test results correlate well with theoretical predictions.